ELSEVIER

Journal of Alloys and Compounds 434–435 (2007) 190–193

Journal of ALLOYS AND COMPOUNDS

www.elsevier.com/locate/jallcom

Glass formability and thermal stability of Al–Ni–Y–Be amorphous alloys

Joong-Hwan Jun *, Jeong-Min Kim, Ki-Tae Kim, Woon-Jae Jung

Light Materials Team, Advanced Materials Division, Korea Institute of Industrial Technology, 994-32 Dongchun-dong, Yeonsu-gu, Incheon 406-800, South Korea

Available online 29 September 2006

Abstract

In this study, the role of Be in glass forming ability (GFA) and thermal stability of $(Al_{85}Ni_7Y_8)_{100-x}Be_x$ ($x = 0$–6 at.%) amorphous alloys has been investigated in an attempt to understand small atomic size effect in Al–TM–RE (TM: transition metal, RE: rare earth metal) alloy system. The supercooled liquid region ($\Delta T_x = T_x - T_g$, where T_x and T_g are the onset crystallization and the glass transition temperatures, respectively), reduced glass transition temperature ($T_{rg} = T_g/T_L$, where T_L is the liquidus temperature), K ($=(T_x - T_g)/(T_L - T_x)$), γ ($=T_x/(T_g + T_L)$) and the activation energy for primary crystallization (E_a), became slightly increased by the addition of 2% Be. The higher GFA representing parameters and thermal stability for the $(Al_{85}Ni_7Y_8)_{98}Be_2$ alloy, however, did not result in a practically enhanced glass formability.
© 2006 Elsevier B.V. All rights reserved.

Keywords: Metallic glasses; Microstructure; Phase transitions

1. Introduction

Al-based amorphous alloys possessing superior specific strength in combination with good ductility, have gained an increasing attention due to their potential applications in structural fields [1,2]. Among them, Al–TM–RE system (TM: transition metal, RE: rare earth metal) such as Al–Ni–Y [3], Al–Ni–Co–Y [4], Al–Ni–Gd [5] and Al–Ni–Fe–Gd [6] has a much better glass forming ability (GFA), which is mainly originated from strong interaction and peculiar atomic configuration between Al and TM atoms [7,8]. In 1990, Inoue et al. [4] introduced an $Al_{85}Ni_5Co_2Y_8$ alloy with high tensile fracture strength (σ_f) and wide supercooled liquid region (ΔT_x) of 1250 MPa and ~35 K, respectively. In spite of numerous subsequent works on Al–TM–RE-based alloys, however, bulk metallic glass former has not been produced so far. This may well be caused by unique characteristics of the Al–TM–RE system such that it can be quenched into amorphous phase only in Al-rich eutectic composition usually over 80 at.% of Al and that the reduced glass transition temperature (T_{rg}) values are generally less than ~0.5, which are quite lower than typical values of 0.6–0.7 for easy glass formers. Recently, Poon et al. [9] have studied the role of large size alkali metals on thermal stability and GFA of $Al_{87}Ni_7Gd_{8-x}$(Ca, Sr, Ba)$_x$ ($x = 1$–3 at.%) alloys, and reported that the addition of larger size elements to replace Gd enhances the thermal stability of the quenched amorphous phase but does not lead to an improved GFA due to the decreased chemical interaction between (Ca, Sr or Ba) and Al.

In the present study, the influence of Be addition on thermal stability and GFA of $Al_{85}Ni_7Y_8$ alloy is investigated in an attempt to understand smaller atomic size effect in Al–TM–RE alloy system. Be was selected as an additional element, after considering its quite smaller atomic radius of 1.12 Å than pre-existing Ni (1.24 Å), Al (1.43 Å) and Y (1.78 Å) as well as its negative heat of mixing with Ni (−4 kJ/mol atom) and Y (−32 kJ/mol atom).

2. Experimental

Four $(Al_{85}Ni_7Y_8)_{100-x}Be_x$ ($x = 0$, 2, 4, 6 at.%) ingots were prepared by arc melting a mixture of Al (99.99%), Ni (99.9%), Y (99.9%) and Al–Be alloyed material in a purified Ar atmosphere. From the master alloy ingots, ribbons with a size about $0.02(t)$ mm × $3(w)$ mm were prepared by means of a single roller melt-spinning technique in an Ar atmosphere. Amorphous nature of the melt-spun ribbons was verified by X-ray diffractometry (XRD, Rigaku CN-2301) with a monochromatic Cu Kα radiation. The thermal properties of the samples such as glass transition temperature (T_g) and onset crystallization temperature (T_x) were determined by differential scanning calorimetry (DSC, Perkin-Elmer DSC-7) with a heating rate of 0.67 K/s under flowing purified Ar. The melting temperature range ($T_m \sim T_L$, where T_m and T_L are melting temperature and liquidus temperature, respectively) was measured by differential thermal analysis (DTA, Perkin-Elmer DTA-7) with a heating rate of 0.33 K/s. The thermal stability associated with the effective activation energy for primary crystallization (E_a) was investigated using a Kissinger plot

* Corresponding author. Tel.: +82 32 8500 425; fax: +82 32 8500 410.
E-mail address: jhjun@kitech.re.kr (J.-H. Jun).

0925-8388/$ – see front matter © 2006 Elsevier B.V. All rights reserved.
doi:10.1016/j.jallcom.2006.08.120

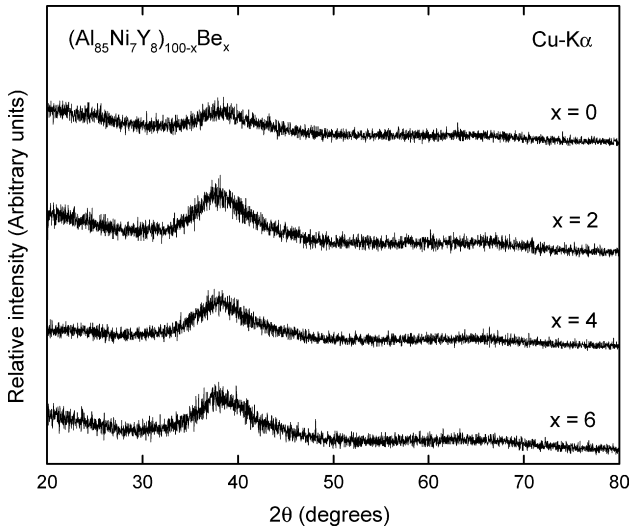

Fig. 1. XRD patterns obtained from Al–Ni–Y–Be alloy ribbon samples.

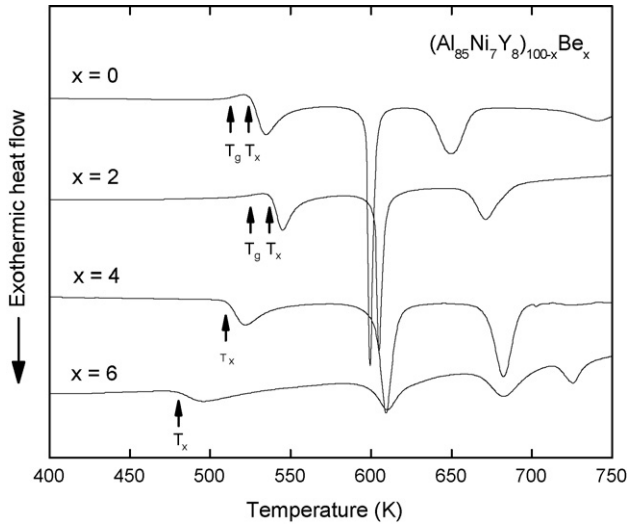

Fig. 2. DSC traces obtained from Al–Ni–Y–Be alloy ribbon samples with a heating rate of 0.67 K/s.

[10]. Hardness of the ribbon sample was measured by using a microvickers hardness tester (Matsuzawa MXT-α) with a load of 100 gf.

3. Results

Fig. 1 represents the XRD traces taken from the melt-spun $(Al_{85}Ni_7Y_8)_{100-x}Be_x$ ($x = 0$, 2, 4, 6 at.%) samples. All XRD patterns show a broad diffraction peak in the 2θ range of 32–50°, reflecting the characteristic of an amorphous structure. This result demonstrates no change in amorphous nature of $Al_{85}Ni_7Y_8$ alloy by the addition of Be up to 6%. The DSC traces of the melt-spun ribbons taken using a heating rate of 0.67 K/s are given in Fig. 2. As well is known, amorphous alloy exhibits an endothermic heat event of the glass transition followed by characteristic exothermic heat release events corresponding to the successive transformations from a supercooled liquid to the equilibrium crystalline phases at different temperatures. The glass transition followed by a supercooled liquid region is observed in the Al–Ni–Y–Be alloys containing Be up to 2%, but it disappears in the alloys with higher Be content. It is noticeable that after adding 2% Be, T_g, T_x and the supercooled liquid region (ΔT_x) defined as ($T_x - T_g$), increase from 514, 523 and 12 to 526, 538 and 15 K, respectively. The T_g, T_x and ΔT_x of the experimental alloys are summarized in Table 1. Fig. 3 shows the DTA traces of the Al–Ni–Y–Be alloys obtained at a heating rate of 0.33 K/s. In all samples, a sharp endothermic peak with an extended tail is observed, suggesting that the Al–Ni–Y–Be alloys are not at an eutectic composition. With increasing Be content, the melting temperature (T_m) and liquidus temperature (T_L) are decreased slightly up to 2% Be and then nearly saturated. The temperature intervals are almost same regardless of Be content. The obtained T_m and T_L values as well as the calculated reduced glass transition temperature ($T_{rg} = T_g/T_L$), K ($=(T_x - T_g)/(T_L - T_x)$) [11] and γ ($=T_x/(T_g + T_L)$) [12] parameters are also given in Table 1. It is noteworthy that all GFA representing parameters (ΔT_x, T_{rg}, K and γ) are higher in the $(Al_{85}Ni_7Y_8)_{98}Be_2$ alloy than those in the basic $Al_{85}Ni_7Y_8$ alloy.

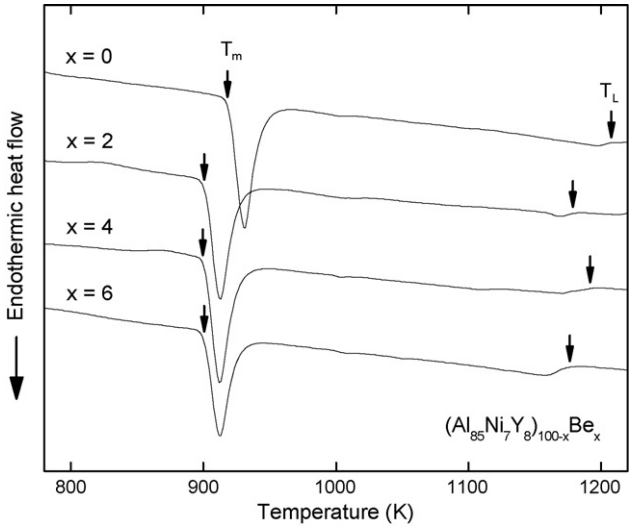

Fig. 3. DTA traces obtained from Al–Ni–Y–Be alloy ribbon samples with a heating rate of 0.33 K/s.

Table 1
The thermal properties (T_x, T_g, T_m and T_L) and GFA indexing parameters (ΔT_x, T_{rg}, K and γ) for Al–Ni–Y–Be alloys

Alloy	T_g (K)	T_x (K)	T_m (K)	T_L (K)	ΔT_x (K)	T_{rg}	K	γ
$Al_{85}Ni_7Y_8$	514	526	916	1206	12	0.436	0.018	0.306
$(Al_{85}Ni_7Y_8)_{98}Be_2$	523	538	898	1179	15	0.456	0.023	0.316
$(Al_{85}Ni_7Y_8)_{96}Be_4$	–	509	898	1190	–	–	–	–
$(Al_{85}Ni_7Y_8)_{94}Be_6$	–	480	896	1175	–	–	–	–

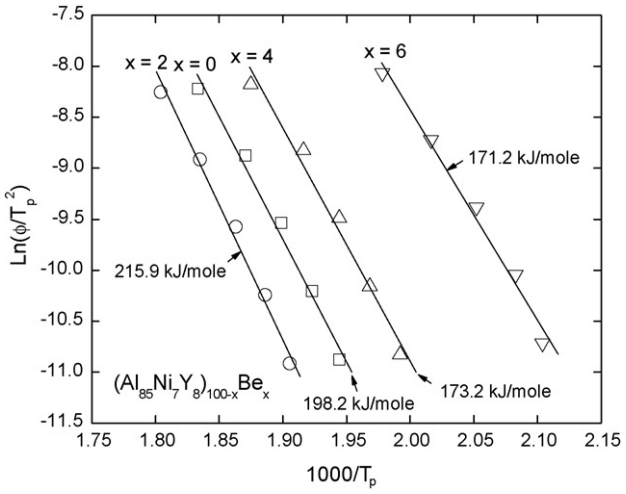

Fig. 4. Kissinger plot of the primary crystallization temperature for Al–Ni–Y–Be alloys.

In order to examine the thermal stability associated with crystallization kinetics for the Al–Ni–Y–Be alloys, the change in $\ln(\phi/T_p^2)$ is plotted as a function of $1000/T_p$ in Fig. 4 in accordance with Kissinger relationship [10], where ϕ and T_p are heating rate and primary crystallization temperature, respectively. The slope corresponds to the effective activation energy for primary crystallization (E_a) and exhibits a peak value of 215.9 kJ/mol for the $(Al_{85}Ni_7Y_8)_{98}Be_2$ alloy, which is moderately higher than 198.2 kJ/mol for the $Al_{85}Ni_7Y_8$ alloy. This implies that the thermal stability of Al–Ni–Y amorphous phase is improved by the 2% Be addition.

Fig. 5 shows the change in microvickers hardness with Be content in the Al–Ni–Y–Be alloys. It is easily observed that the hardness decreases slightly up to 2% Be, over which it deteriorates steeply. The XRD patterns taken from the cross-sections of the injection-cast $Al_{85}Ni_7Y_8$ and $(Al_{85}Ni_7Y_8)_{98}Be_2$ alloys with 1mm in diameter are represented in Fig. 6. Both alloys contain several diffraction peaks corresponding to crystalline phases, but

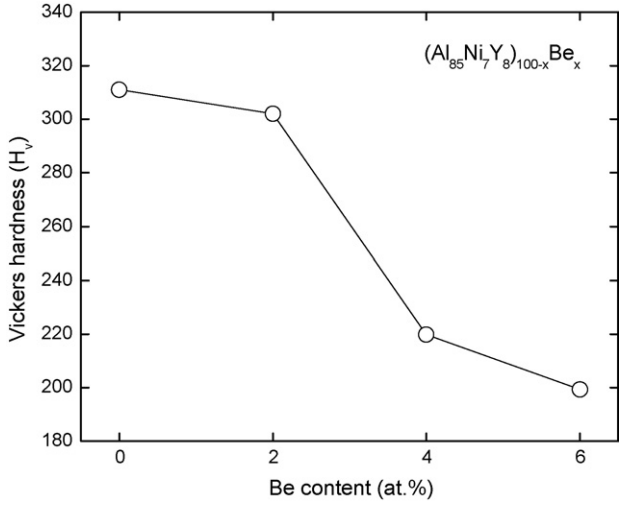

Fig. 5. Variation in microvickers hardness with Be content in Al–Ni–Y–Be alloy ribbon samples.

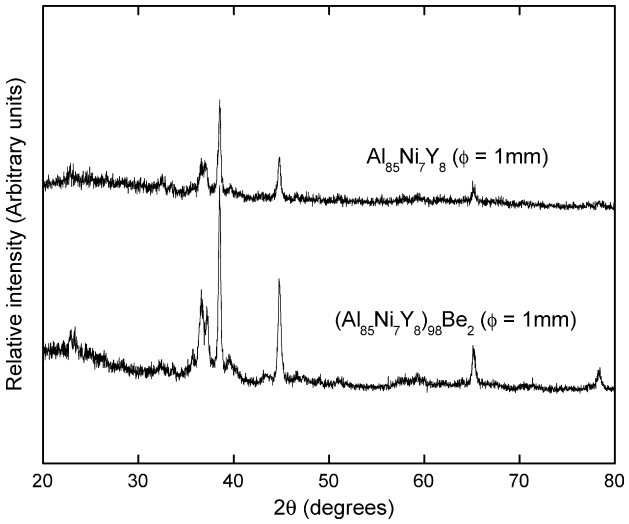

Fig. 6. XRD patterns obtained from $Al_{85}Ni_7Y_8$ and $(Al_{85}Ni_7Y_8)_{98}Be_2$ injection-cast rod samples with 1 mm in diameter.

intensities of the peaks are greater in the $(Al_{85}Ni_7Y_8)_{98}Be_2$ than in the $Al_{85}Ni_7Y_8$ alloy. The results shown in Figs. 5 and 6 indicate that the $(Al_{85}Ni_7Y_8)_{98}Be_2$ alloy does not possess a better GFA practically than $Al_{85}Ni_7Y_8$ alloy, although simultaneous increase in thermal stability and GFA indexing parameters (ΔT_x, T_{rg}, K and γ) is attained by the addition of 2% Be.

4. Discussion

A higher order multicomponent system, a significant atomic size difference between alloying elements and a large negative heat of mixing between the elements have been recognized as three qualitative glass forming criteria [13,14].

Considering the shift of T_x from 526 to 538 K (Table 1) and increased E_a from 198.2 to 215.9 kJ/mol by the 2% Be addition (Fig. 4), the amorphous phase of $(Al_{85}Ni_7Y_8)_{98}Be_2$ alloy is believed to have higher thermal stability than $Al_{85}Ni_7Y_8$ alloy. Moreover, various GFA indexing parameters such as ΔT_x, T_{rg}, K and γ for the $Al_{85}Ni_7Y_8$ alloy are increased by the 2% Be addition from 12 K, 0.436, 0.018 and 0.306 to 15 K, 0.456, 0.023 and 0.316, respectively (Table 1). The increased thermal stability and GFA indexing parameters for the $(Al_{85}Ni_7Y_8)_{98}Be_2$ alloy, however, does not result in a practically improved GFA, as observed in Figs. 5 and 6.

In a previous work, Poon et al. [9] reported that the thermal stability is associated with solid-state atomic diffusion and that higher packing density of the Al-based amorphous phase attained by an addition of alloying elements with large atomic size difference can give rise to the improvement in thermal stability, even though it might lower the chemical interaction between alloying elements. In case of the GFA, however, they explained that it has a strong dependence on chemical interaction between Al and other elements rather than packing density or atomic size difference. After considering that the negative heat of mixing (ΔH_{mix}) values between Al and other elements in Al–Ni–Y system are −22, −38 and −31 kJ/mol atom for Al–Ni, Al–Y and Ni–Y, respectively, and that the ΔH_{mix} values

concerning Be are 0, −4 and −32 kJ/mol atom for Al–Be, Ni–Be and Y–Be, respectively, it is reasonable to expect that the higher the Be content in the Al–Ni–Y system, the lower the chemical interaction between Al and other alloying elements. As for the Al–Ni–Gd–(Ca, Sr, Ba) system [9], the increased thermal stability for the $(Al_{85}Ni_7Y_8)_{98}Be_2$ alloy is understood that the higher packing density by the 2% addition of Be with smaller atomic size might compensate the decrease in thermal stability due to the reduced bonding forces. The reason for the increase in GFA parameters in the $(Al_{85}Ni_7Y_8)_{98}Be_2$ alloy is not clear at present, but it could be explained by the increased thermal stability.

The decreased hardness and greater intensities of the crystalline peaks in the XRD pattern for the $(Al_{85}Ni_7Y_8)_{98}Be_2$ alloy (Figs. 5 and 6) clearly indicate that the increase in thermal stability and GFA representing parameters does not result in the practically enhanced glass formability of the Al–Ni–Y alloy. It strongly demonstrates that the chemical interaction between Al and other components plays an essential role in the practical glass formability for the Al-based alloys.

5. Summary

The GFA and thermal stability of the $(Al_{85}Ni_7Y_8)_{100-x}Be_x$ ($x = 0$–6 at.%) amorphous alloys were studied to understand small atomic size effect in Al–TM–RE alloy system. The T_x and E_a become higher for the $(Al_{85}Ni_7Y_8)_{98}Be_2$ alloy, indicating that the thermal stability of the $Al_{85}Ni_7Y_8$ alloy is enhanced by the addition of 2% Be. The GFA indexing parameters such as ΔT_x, T_{rg}, K and γ are also increased slightly after 2% Be addition. The increased thermal stability of the $(Al_{85}Ni_7Y_8)_{98}Be_2$ alloy is believed that higher packing density by the 2% addition of Be with smaller atomic size might compensate the decrease in thermal stability due to the reduced bonding forces, which eventually might lead to the increase in GFA representing parameters. The increased parameters concerning GFA and thermal stability by the 2% Be addition, however, does not lead to a practically enhanced glass formability. It implies that the chemical interaction between Al and other alloying elements plays an essential role in the practical GFA for the Al-based alloys.

References

[1] A. Inoue, Prog. Mater. Sci. 43 (1998) 365.
[2] Y. He, S.J. Poon, G.J. Shiflet, Science 241 (1988) 1640.
[3] A. Inoue, K. Ohtera, A.P. Tsai, T. Masumoto, Jpn. J. Appl. Phys. 27 (1988) L479.
[4] A. Inoue, N. Matsumoto, T. Masumoto, Mater. Trans. JIM 31 (1990) 493.
[5] F. Guo, S.J. Poon, G.J. Shiflet, Scripta Mater. 32 (2000) 1089.
[6] Y. He, G.M. Dougherty, G.J. Shiflet, S.J. Poon, Acta Metall. 41 (1993) 337.
[7] A.N. Mansour, C.P. Wong, R.A. Brizzolara, Phys. Rev. B 50 (1994) 12401.
[8] H.Y. Hsieh, B.H. Toby, T. Egami, Y. He, S.J. Poon, G.J. Shiflet, J. Mater. Res. 5 (1990) 2807.
[9] F. Guo, S. Enouf, G.J. Shiflet, S.J. Poon, Mater. Trans. JIM 41 (2000) 1406.
[10] H.E. Kissinger, Anal. Chem. 29 (1957) 1411.
[11] A. Hruby, Czech. J. Phys. B22 (1972) 1187.
[12] Z.P. Lu, C.T. Liu, Acta Mater. 50 (2002) 3501.
[13] S.G. Kim, A. Inoue, T. Masumoto, Mater. Trans. JIM 31 (1990) 929.
[14] A. Peker, W.L. Johnson, Appl. Phys. Lett. 63 (1993) 2342.